Expression of *salinarum* halorhodopsin in *Escherichia coli* cells: solubilization in the presence of retinal yields the natural state

Yasutaka Yamashita[a], Takashi Kikukawa[a,*], Takashi Tsukamoto[a], Masakatsu Kamiya[a], Tomoyasu Aizawa[a], Keiichi Kawano[a], Seiji Miyauchi[b], Naoki Kamo[c], Makoto Demura[a]

[a]Faculty of Advanced Life Science, Hokkaido University, Sapporo 060-0810, Japan

[b]Graduate School of Pharmaceutical Sciences, Toho University, Funabashi, Chiba 274-8510, Japan

[c]College of Pharmaceutical Sciences, Matsuyama University, Matsuyama, Ehime 790-8578, Japan

[*]Corresponding author:

Tel: +81-11-706-3435; Fax: +81-11-706-2771; E-mail address: kikukawa@sci.hokudai.ac.jp

Postal address: Faculty of Advanced Life Science, Hokkaido University, N10W8, Kita-ku, Sapporo 060-0810, Japan

ABSTRACT

Salinarum halorhodopsin (HsHR), a light-driven chloride ion pump of haloarchaeon *Halobacterium salinarum*, was heterologously expressed in *Escherichia coli*. The expressed HsHR had no color in the *E. coli* membrane, but turned purple after solubilization in the presence of all-*trans* retinal. This colored HsHR was purified by Ni-chelate chromatography in a yield of 3-4 mg per liter culture. The purified HsHR showed a distinct chloride pumping activity by incorporation into the liposomes, and showed even in the detergent-solubilized state, its typical behaviors in both the unphotolyzed and photolyzed states. Upon solubilization, HsHR expressed in the *E. coli* membrane attains the proper folding and a trimeric assembly comparable to those in the native membranes.

Keywords:

Archaeal rhodopsin; Halorhodopsin; Light-driven chloride pump; Photocycle

Abbreviations:

HsHR, halorhodopsin from *Halobacterium salinarum*; HR, halorhodopsin; NpHR, HR from *Natronomonas pharaonis*; BR, bacteriorhodopsin; NpSRII, sensory rhodopsin II from *Natronomonas pharaonis*; IPTG, isopropyl-β-D-thiogalactopyranoside; DDM, n-dodecyl β-D-maltopyranoside; MES, 2-(N-morpholino)ethanesulfonic acid; CCCP, carbonyl cyanide m-chlorophenylhydrazone.

1.Introduction

Halorhodopsin (HR) is a light-driven Cl^- ion pump originally found in the cell membrane of haloarchaeon, *Halobacterium salinarum* [1-4]. Like other microbial rhodopsins, the light-induced isomerization of retinal, bound to a specific lysine residue *via* the protonated Schiff base, triggers the cyclic photoreaction of HR termed a "photocycle" [5, 6]. HR then accomplishes the Cl^- translocation from the outside to the inside of the cell. Since its original discovery from *H. salinarum*, many HR homologues from different sources have been reported. However, most studies to date have been conducted using two HRs; i.e., the original HR from *H. salinarum* (HsHR) and HR from *Natronomonas pharaonis* (NpHR). Besides HsHR, *H. salinarum* also contains light-driven H^+ pump bacteriorhodopsin (BR), which creates a proton gradient used for the ATP synthesis [7]. The other pump, HsHR, mainly contributes to maintaining the high salt concentration in the cell interior [8]. On the other hand, *N. pharaonis*, an inhabitant under alkaline conditions, lacks BR. In this strain, NpHR mainly contributes to the light-driven ATP synthesis like BR in *H. salinarum* [9, 10].

These HsHR and NpHR have the same global fold and high similarities in the amino acid sequences (identity, 66%; homology, 97%). However, profound differences exist in both of their unphotolyzed and photolyzed states. The representative examples are as follows: 1) The Cl^--binding to unphotolyzed HsHR results in a rather small red shift of the visible absorption spectra [11-13], while NpHR shows a large blue shift (~20 nm) [14, 15]. 2) The retinal isomeric composition of the

unphotolyzed HsHR changes depending on the light- and dark-adaptation conditions [13, 16]. This adaptation does not occur in NpHR [15]. 3) In both proteins, Cl^- bound in the vicinity of the protonated Schiff base is believed to be transported during the photocycles [17-19]. Besides this primal Cl^-, HsHR has another Cl^- binding site consisting of Arg 24, Arg 103 and Gln 105 near the extracellular surface [18]. NpHR does not preserve these residues and probably lacks this second Cl^- binding site. 4) NpHR has the longest B-C loop among most of the microbial rhodopsins. As compared to HsHR, the extra 10 residues are inserted in the loop of NpHR and form a characteristic "cap" covering the extracellular surface of this protein [19]. 5) There are distinct differences in both photocycles in the presence and absence of Cl^- [13, 15, 20, 21]. HsHR binding with Cl^- undergoes the photocycle lacking the O-intermediate, which is clearly observed in the NpHR photocycle. Furthermore, the photocycle of HsHR unbinding with Cl^- includes only the intermediates absorbing long wavelengths, while the corresponding photocycle of NpHR additionally includes the other intermediate absorbing short wavelengths. 6) The specificities for the transportable anions seem different [22]. For HsHR, the transport efficiency for NO_3^- is about 30% for Cl^-. For NpHR, both ions are transported at almost the same efficiency. For a better understanding of their Cl^- transport mechanisms, the molecular origins of these differences as well as the consequences of their structural differences should be clarified. However, there are only a few comparative studies of this, likely due to the lack of a facile sample preparation system for HsHR.

After the first success of the recombinant expression of the *N. pharaonis* sensory rhodopsin II (NpSRII) [23], which is a light sensor for a negative phototaxis, the *E. coli* expression system has been examined for many microbial rhodopsins and widely used. For NpHR, a large amount of this protein was shown to be functionally expressed in the *E.coli* membrane [24, 25], and so the studies using various NpHR mutants have been facilitated [26-34]. For HsHR, however, its *E. coli* expression has not yet been reported, and only several mutants were studied using the *H. salinarum* recombinant system [18, 20, 35].

In this study, we attempted the expression of HsHR in the *E. coli* cell. Although HsHR was not functionally expressed in the *E. coli* membrane, it became colored upon detergent solubilization in the presence of the all-*trans* retinal. The purified HsHR showed almost the same behaviors as HsHR in the native membrane. To the best of our knowledge, this is the first functional purification of HsHR from *E. coli* cells.

2. Materials and Methods

2.1 Expression and purification of HR from E. coli cells

Escherichia coli DH5α was used as the host for the DNA manipulation. To isolate HsHR gene, PCR was employed using the *H. salinarum* genomic DNA. Two PCR primers were designed so that a *Nde*I site was engineered at the initiation codon, and a 6 × histidine tag and a *Xho*I site were

inserted before and after the stop codon, respectively. The used sense and antisense primers were 5'-TCTACATATGTCAATCACGAGTGTACCCGGTG-3' and 5'-TATACTCGAGTCAGTGGTGGTGGTGGTGGTGGTCGTCGCTTGACATGGTGCCAAG-3', respectively, in which the underlines denote *Nde*I, the *Xho*I sites and histidine tag region. The PCR product was then restricted, and the resultant DNA fragments were ligated to the *Nde*I/*Xho*I site of pET-21c (+) (Novagen, Madison, WI). The DNA sequence was confirmed by a standard procedure using an automated DNA sequencer (model 3100, Applied Biosystems, Foster City, CA). The obtained plasmid was called pET-HsHRHis. This has essentially the same construct as the expression plasmid for NpHR as previously described [25].

The expression and purification procedure of the histidine-tagged NpHR has been described in detail elsewhere [25]. Briefly, *E. coli* BL21(DE3) cells harboring the expression plasmid were grown at 37 °C in 2 × YT medium supplemented with ampicillin (50 μg/mL). Three hours after the 1 mM isopropyl-β-D-thiogalactopyranoside (IPTG) induction with the addition of 10 μM all-*trans* retinal, violet-colored cells were harvested by centrifugation (6,400 × g, 8 min at 4 °C) and disrupted by a French press (Ohtake, Tokyo, Japan) (100 MPa × 4 times). After removing the insoluble fraction by centrifugation (5,600 × g, 10 min at 4 °C), the supernatant was ultracentrifuged (178,000 × g, 90 min at 4 °C). The collected membrane fraction was then solubilized with 1.5% n-dodecyl β-D-maltopyranoside (DDM) (Dojindo Lab, Kumamoto, Japan) in 50 mM MES, pH 6.5, including

300 mM NaCl and 5 mM Imidazole, and the solubilized NpHR was purified by Ni-NTA-agarose (Qiagen, Hilden, Germany) in the presence of 0.1% DDM. The samples were then replaced by the appropriate buffer solution by two passages over a PD-10 column (Amersham Bioscience, Uppsala, Sweden). For HsHR, the same procedures as for the NpHR were first examined, but modifications were required for the host strain to Rosetta(DE3) (Novagen, Madison, WI) and the solubilization conditions. These details are described in section 3.1.

To examine the protein expression, SDS-PAGE and Western blot analyses were performed on the individual fractions of the *E. coli* cells. The proteins were separated by SDS-PAGE with 4% acrylamide stacking and 12% acrylamide separating gels, and then visualized with InVision His-tag in-gel stain (Invitrogen, Carlsbad, CA) or further analyzed by Western blot using the anti-histidine tag monoclonal antibody.

2.2 Preparation of H. salinarum membranes expressing HsHR

For the expression of HsHR in *H. salinarum*, the plasmid was constructed by modification of the pJS010 plasmid that encodes the fusion gene of NpSRII and its cognate transducer [36]. Its original *Nco*I site at the initiation codon was replaced with *Nde*I using the QuikChange site-directed mutagenesis kit (Stratagene, La Jolla, CA). The resultant *Nde*I/*Xho*I region was then replaced with the corresponding region of pET-HsHRHis encoding the histidine-tagged HsHR. According to the

previously reported protocol [37], the obtained plasmid was introduced into the *H. salinarum* strain Pho81Wr$^-$ [38], which lacks the four archaeal rhodopsins, and the transformants were grown in the presence of 4 μM mevinolin.

The membranes expressing HsHR were prepared while maintaining a high ionic strength equivalent to 4 M NaCl as follows. The cells were harvested at 6,400 × g for 15 min at 4 °C and washed twice with 4 M NaCl buffer (10 mM MES, pH 6.0), and then disrupted by a French press at 100 MPa × 8 times. After removing the undisrupted cells by centrifugation (6,400 × g for 15 min at 4 °C), the supernatant was ultracentrifuged at 178,000 × g for 90 min at 4 °C and washed twice with the same 4 M NaCl buffer. The flash-photolysis experiments were performed using this membrane fraction in the presence or absence of Cl^-. The latter Cl^--free sample was prepared by dialysis against 1.33 M Na_2SO_4 including 10 mM MES, pH 6.0.

2.3 Flash-photolysis spectroscopy

The details of the flash-photolysis apparatus were previously reported [28]. The transient absorption changes induced by a laser pulse (Nd:YAG, 532 nm, 7 ns, 5 mJ／pulse) were recorded in a computer at every 0.5 μs between -44 and 220 ms. At each selected measuring wavelength (every 10 nm from 400 to 750 nm), 30 laser pulses were used to improve the S／N ratio. The data points were then selected by choosing a logarithmic time scale to reduce the number of points. All

measurements were performed at 20 °C. For the measurements using the intact *E.coli* cells expressing NpHR and HsHR, the cells were used after washing and resuspending with a buffer solution containing 300 mM NaCl and 10 mM MES, pH 7.0. The cell densities were adjusted in order to be identical using OD_{660}.

2.4 Absorption and CD spectra measurements

The absorption spectra were measured by a spectrometer (Model BioSpec-mini Shimadzu, Kyoto, Japan). The CD spectrum of HsHR was measured by a Jasco J-725 spectropolarimeter (Jasco, Tokyo, Japan) in the 400-700 nm region at 25 °C at a scanning speed of 200 nm/min, and the accumulation was carried out twice.

2.5 Gel filtration chromatography

The purified NpHR and HsHR were applied to a Superdex 200 5/150 GL size exclusion column as previously described [34]. Standards for the calibration of the molecular mass were Blue Dextran 2000 (2,000,000 Da,Pharmacia), Ferritin (horse spleen, 440,000 Da, Pharmacia), Aldolase (rabbit muscle, 158,000 Da, Pharmacia), Albumin (bovine serum, 66,000, Sigma) and Lysozyme (chicken egg white, 14,313 Da, Sigma). All chromatographs were obtained at room temperature with 10 mM MES, pH 6.0, including 300 mM NaCl and 0.1% DDM. The eluting proteins were monitored

at 280, 340 and 580 nm, and then the molecular weights of the HRs-DDM complexes were estimated by the standard method.

2.6 Light-enhanced bleaching of NpHR and HsHR

The bleaching rates of the two purified HRs from the *E. coli* membrane were examined under a desalted condition, 10 mM MES, pH 6.0, including 0.1% DDM. Two HRs were continuously irradiated at room temperature by a 650-Watt halogen lamp after passing through a Y52 filter (Toshiba, Tokyo, Japan) and a $CuSO_4$ solution. The time courses of the absorbance changes at their respective λ_{max}s (577 nm for HsHR, 600 nm for NpHR) were monitored by the spectrophotometer.

2.7 Analysis of retinal isomer composition

Before the retinal extractions, HsHR was dark adapted by storage in the dark for 10 days in 10 mM MES, pH 6.0, including 300 mM NaC1 and 0.1% DDM. For light-adaptation, it was irradiated for 5 min by yellow light from a 650-Watt halogen lamp described above. After methanol and hydroxylamine were added to each of the dark- and light-adapted HsHR solutions, the retinal oximes were extracted with hexane and subjected to an HPLC system consisting of a LC-10AT pump and SPD-10AV UV/Vis detector (Shimadzu, Kyoto, Japan). The details were described

elsewhere [39].

2.8 Functional reconstitution into asolectin liposomes

The reconstitution was performed according to previous reports with some modifications [40, 41]. Asolectin (Sigma, St. Louis, MO) was twice purified by acetone/diethyl ether fractionation cycles, and then stored by dissolving in chloroform (100 mg/mL) at -20 °C. The desired amount of the chloroform solution was evaporated in a stream of nitrogen and dried under vacuum for at least 3 h. The resultant lipid film was dispersed using a bath-type sonicator in 0.1 mM MES, pH 6.0, including 1 M NaCl. This lipid suspension was then mixed with the same volume of purified HsHR, which was dispersed in the same buffer supplemented with 0.05% DDM. The lipid/protein ratio was 270 : 1 (w/w). The amount of HsHR was calculated using the extinction coefficient of 50,000 $M^{-1}cm^{-1}$ at λ_{max} [42]. After a 1-h incubation at 25 °C with gentle shaking, the detergent in the mixture was slowly removed by adding 50 mg of Bio-Beads every 6 h. This detergent removal was extended for at least 36 h. After removal of the Bio-Beads, the suspension was briefly centrifuged at 1,000 × g for 10 min to remove the large lipid aggregate. The residual supernatant was used for the subsequent measurement of the Cl^- pumping activity.

Chloride transport by HsHR was examined as previously described [40, 41]. The transport was detected by following the light-induced pH changes that originate from the passive proton movement in response to the membrane potential created by the chloride transport. The proteoliposomes in the

magnetically-stirred 10-mm optical cuvette was irradiated by orange light (590 ± 8.5 nm) from a high power LED (LXHL-LL3C, Philips Lumileds Lighting Co., San Jose, CA). The transport was examined in the absence and presence of 50 μM carbonyl cyanide m-chlorophenylhydrazone (CCCP) and 1% DDM. The typical sample volume was 1.5 mL and the measurements were performed at room temperature. The obtained pH changes were standardized after each measurement by adding known amounts of HCl.

3. Results and Discussion

3.1 Expression of HsHR in the E. coli cells

The histidine-tagged NpHR is shown to be functionally expressed in the *E. coli* membrane by incorporating the all-*trans* retinal with added IPTG. The yield after the Ni-chelating chromatography is about 20 mg per liter cell culture [25]. Using the same procedure, we attempted the expression of HsHR. Figure 1 A shows the comparison of two expression hosts, BL21(DE3) (lane 1) and Rosetta(DE3) (lane 2); the latter is a rare codon optimizer strain derived from BL21. The whole-cell extracts were separated by SDS-PAGE and visualized with InVision His-tag in-gel stain. An intense band (marked by an arrow), corresponding to HsHR, appears in Rosetta(DE3), but not in BL21(DE3). This difference probably reflects the fact that HsHR gene includes a rare codon cluster in the region from Arg 56 to Arg 60, where 4 out of 6 codons are classified as rare codons. Hereafter,

Rosetta(DE3) was used for HsHR expression.

For NpHR, it is expressed even in BL21(DE3) and the cells are colored violet. Upon the flash irradiation of these cells, the absorbance change shown in Fig. 1 B (upper trace) is observed reflecting the photocycle of NpHR. For HsHR, we extensively examined its expression by varying the IPTG induction timing, IPTG concentration, all-*trans* retinal concentration, induction temperature and period. However, the Rosetta(DE3) cells did not color and showed no flash-induced absorbance change (Fig. 1 B, lower trace). The Western-blot analyses of the Rosetta(DE3) cells are shown in Fig 1 C. The intense band corresponding to HsHR appeared in the whole cell extract (lane 1). This expressed HsHR is not contained in either the insoluble cytoplasmic aggregates (lane 2) or soluble cytoplasmic fraction (lane 3), but was contained in the cell membrane fraction (lane 4). Thus, HsHR was expressed in the *E. coli* membrane as a colorless pigment. The same results were also reported for BR [43]. By the previous studies, BR was shown to become colored after the DDM-solubilization of the membrane fraction [24, 44], suggesting that, in the *E. coli* membrane, BR is binding with the retinal, but is not properly folded. The solubilized BR then becomes able to take the proper conformation. However, this solubilization is not adequate for HsHR. To obtain the colored HsHR, the solubilization was required to be done in the presence of the all-*trans* retinal. Lane 5 of Fig. 1 C shows the band of HsHR purified by Ni-chelating chromatography after this solubilization. The yield of the colored HsHR, which was evaluated after purification, increased with

the increasing retinal concentration during the solubilization process, and then became saturated at about 500 μM retinal. Within the *E. coli* membrane, HsHR probably undergoes the incorrect conformation and cannot bind the retinal. The following solubilization may enable HsHR to bind retinal and to correctly fold. Figure 1 D shows the absorption spectrum of the finally obtained HsHR. As shown later, this purified HsHR shows a spectral change upon light-dark adaptation. In the light-adapted state, its absorption maximum locates around 577 nm and the absorbance ratio at 280 nm to 577 nm is 1.56. These values are close to those of the highly purified HsHR from the native membrane [42, 45]. As calculated using the extinction coefficient of 50,000 $M^{-1}cm^{-1}$ at λ_{max} [42], the average yield of the purified HsHR was about 3-4 mg per liter of cell culture.

3.2 Photostability of the purified HsHR

The solubilized NpHR is known to be stable under various conditions, but to be rather easily bleached by continuous illumination under the desalted condition [46]. We now compared the stabilities of the HRs purified from the *E. coli* membrane. Fig 2 shows their bleaching rates under the desalted condition by the continuous illumination of yellow light. The unbleached (alive) concentrations of the HRs were estimated from the absorbances at the respective λ_{max}s and plotted versus the duration of the illumination. Interestingly, about 60% of the NpHR was bleached by a 4-h irradiation, but for HsHR, only a slight bleaching (~ 2%) was observed. As described above, the two

HRs are known to undergo different photocycles especially in the Cl^--free medium, suggesting the different conformation changes of their photolyzed states. This difference might cause the remarkable difference in the respective stabilities under the desalted condition.

3.3 Analysis of oligomeric state

In the native membrane, HsHR is known to show a characteristic bilobed CD spectrum due to exciton coupling, suggesting the oligomeric state [45]. This observation is consistent with the trimeric assemblies revealed by the X-ray diffractions [17, 18]. Thus, HsHR is thought to intrinsically form a trimer, but this trimeric assembly is disrupted by a rather strong detergent as well as exposing the membrane to a low salt medium [41, 45]. Upon these treatments, the CD spectrum showed a single positive band. Previously, we showed that NpHR purified from the *E. coli* membrane forms a trimer even in the DDM-solubilized state based on the CD spectra, gel-filtration chromatography, SDS-PAGE and mass spectra [34]. We then examined an oligomeric state of the purified HsHR. As shown in Fig. 3 A, the bilobed CD band was observed for HsHR in the DDM-solubilized state. This asymmetric spectrum having a rather small positive band is comparable to that of the purified HsHR from the native membrane [45]. The next concern is how many monomers assemble to form the oligomer. We then compared the gel filtrations of the DDM-solubilized HsHR and NpHR. The two chromatographs were almost superimposable as shown

in Fig. 3 B. These peaks were estimated to be 209 kDa for HsHR and 231 kDa for NpHR. The latter is close to the previous estimation for the NpHR trimer surrounded by the DDM micelle [34]. In the present constructs, the polypeptide of the expressed HsHR is 19 residues shorter than that of NpHR. This difference probably caused the 22 kDa difference in the total masses. These results revealed that the purified HsHR forms a trimer comparable to that of NpHR.

3.4 Cl^--dependent spectral change

We next examined the Cl^- binding to the purified HsHR. Figures 4 A and B show the Cl^--dependent spectral shift and the calculated difference spectra, respectively. The ionic strengths of the solutions were maintained at the constant equivalent of 4 M NaCl by the addition of Na_2SO_4, because sulfate is neither spectrally bound nor transported by HsHR [47]. As the Cl^- concentration increases, the absorption spectrum became narrow and the amplitude increased. Similar spectral changes of HsHR were previously reported [13, 40]. In previous reports, however, the spectral changes were accompanied by about a 10-nm redshift of the absorption maximum [11, 13, 40]. This shift was not observed in our purified HsHR, whose absorption maximum did not change from 577 nm. In the corresponding difference spectra (Fig 4 B), an isosbestic point was observed at 610 nm, indicating a single-step transition of HsHR from the Cl^--unbinding to binding state. The amplitude change at the absorption maximum gives a dissociation constant Kd of 2.6 mM (Fig. 4 C). This

value is eight times lower than that of HsHR in the native membrane (~ 20 mM) [13]. Thus, our purified HsHR is different from that within the native membrane in lacking the spectral redshift and rather strong affinity to Cl^-. These differences might come from the detergent solubilization and/or the composition difference in the boundary lipids.

3.5 Light-dark adaptation

For HsHR, it is known that the isomeric contents of the retinal shifts toward the all-*trans* at the expense of 13-*cis* upon sustained illumination [12, 13]. Such a light-dark adaptation does not occur in NpHR [15]. We investigated whether or not our purified HsHR shows a light-dark adaptation in the presence of 4 M NaCl. After illumination, the purified HsHR showed a spectral redshift from 569 to 577 nm (Fig. 5 A), suggesting an increase in the all-*trans* retinal content [12]. The HPLC analysis shown in Fig. 4 B revealed that the spectral shift accompanies the change in retinal contents from 50% all-*trans* and 50% 13-*cis* in the dark to 86% all-*trans* and 14% 13-*cis* after illumination. These behaviors are very close to that of HsHR in the native membrane [11, 15].

3.6 Photocycle of Cl^--binding and unbinding form

As described above, the unphotolyzed HsHR from the *E. coli* membrane almost retains the native characters even in the DDM-solubilized state. Next, we examined the behaviors of the

photolyzed states from the photocycle kinetics and Cl^--pumping activity. Figure 6 shows the comparisons of the flash-induced absorbance changes of the DDM-solubilized HsHR from the *E. coli* membrane and HsHR in the native membrane. The data at the two salt concentrations, 4 M NaCl or 1.33 M Na_2SO_4, are shown along with the flash-induced difference spectra (left column) and time-dependent absorbance changes at three selected wavelengths (right column). By exposure to a medium of low ionic strength, the trimeric assembly of HsHR in the native membrane was irreversibly disrupted [45]. Thus, we prepared the native membrane fractions by keeping the ionic strengths equivalent to 4 M NaCl, therefore, these fractions mostly include the cell envelope vesicles. We showed the flash-photolysis data in the presence of 0.5% Tween-20, intending to deplete the membrane potential created by the photolyzed HsHR. However, only slight differences were observed after the addition of this detergent (data not shown). In the early time region (~10 μs) with 4 M NaCl (Fig. 6 A), a small positive absorbance change around 650 nm, probably due to the K-intermediate, was observed for the purified HsHR (upper panels) but not for HsHR in the native membrane (lower panels). Except for this small difference, the overall photocycles are almost identical. As observed here, HsHR photocycle is known to include the easily detectable L-intermediate around 500 nm, but lacks the subsequent O-intermediate [13, 20], which is easily observed in the NpHR photocycle around 650 nm [15, 21]. In the absence of Cl^- (Fig 6 B), two HRs also essentially underwent the same photocycles except for the slightly slow kinetics of the purified

HsHR (upper panels). As seen here, HsHR unbinding with Cl^- is known to undergo the photocycle including only the red-shifted intermediates [13, 20]. This is a distinct difference from the corresponding NpHR photocycle, which includes both the red-shifted and blue-shifted intermediates [15, 21].

3.7 Cl^--pumping activity

To test the Cl^--pumping activity of HsHR from the *E. coli* membrane, we reconstituted them into asolectin liposomes. As shown in the left trace of Fig. 7, the illumination caused a distinct extra-medium acidification, which was facilitated in the presence of CCCP (data not shown). This indicates the passive proton extrusion in response to the membrane potential created by the active Cl^- transport of HsHR. As found in previous reports about HsHR and BR [40, 41], extra-medium acidification means that HsHR is preferentially oriented in the opposite direction to that in the native cell membrane. As shown in the right trace in Fig. 7, the further addition of 1% DDM, which does not denature HsHR (data not shown), completely abolished the medium acidification, again supporting the transmembrane Cl^- transport by the photolyzed HsHR.

4. Conclusions

In contrast to NpHR, HsHR was not functionally expressed in the *E. coli* membrane, but

turned purple after DDM-solubilization in the presence of the all-*trans* retinal. The highly purified HsHR was successfully obtained by Ni-chelating chromatography. The purified HsHR showed the following features: (1) high stability under the low salt condition; (2) almost native behaviors in both the unphotolyzed and photolyzed states even in the DDM-solubilized environment; and (3) distinct Cl^--pumping activity in the reconstituted liposomes. Thus, these results provide useful tools for the preparation of HsHR mutants, and for the consequent facilitation of comparative studies between HsHR and NpHR.

Acknowledgements

We thank Prof. John L. Spudich, at the University of Texas-Houston Medical School, for providing the pJS010 plasmid and Pho81Wr$^-$ strain. This study was supported by a grant from the Japanese Ministry of Education, Culture, Sports, Science, and Technology to T.K. (23510251).

References

[1] A. Matsuno-Yagi, Y. Mukohata, ATP synthesis linked to light-dependent proton uptake in a red mutant strain of Halobacterium lacking bacteriorhodopsin, Arch. Biochem. Biophys. 199 (1980) 297-303.

[2] B. Schobert, J.K. Lanyi, Halorhodopsin is a light-driven chloride pump, J. Biol. Chem. 257 (1982) 10306-10313.

[3] E. Bamberg, P. Hegemann, D. Oesterhelt, The chromoprotein of halorhodopsin is the light-driven electrogenic chloride pump in *Halobacterium halobium*, Biochemistry 23 (1984) 6216-6221.

[4] J.K. Lanyi, Halorhodopsin, a light-driven electrogenic chloride-transport system, Physiol. Rev. 70 (1990) 319-330.

[5] G. Váró, Analogies between halorhodopsin and bacteriorhodopsin, Biochim. Biophys. Acta 1460 (2000) 220-229.

[6] J.L. Spudich, K.-H. Jung, Microbial rhodopsin: Phylogenetic and functional diversity, in: W.R. Briggs, J.L. Spudich (Eds.), Handbook of photosensory receptors, Wiley-VCH Verlag, Weinheim, 2005, pp. 1-23.

[7] D. Oesterhelt, W. Stoeckenius, Functions of a new photoreceptor membrane, Proc. Natl. Acad. Sci. USA 70 (1973) 2853-2857.

[8] A. Duschl, G. Wagner, Primary and secondary chloride transport in *Halobacterium halobium*, J. Bacteriol. 168 (1986) 548-552.

[9] A.V. Avetisyan, A.D. Kaulen, V.P. Skulachev, B.A. Feniouk, Photophosphorylation in alkalophilic halobacterial cells containing halorhodopsin: chloride-ion cycle?, Biochemistry (Moscow) 63 (1998) 625-628.

[10] M. Falb, F. Pfeiffer, P. Palm, K. Rodewald, V. Hickmann, J. Tittor, D. Oesterhelt, Living with two extremes: conclusions from the genome sequence of *Natronomonas pharaonis*, Genome Res. 15 (2005) 1336-1343.

[11] T. Ogurusu, A. Maeda, N. Sasaki, T. Yoshizawa, Effects of chloride on the absorption spectrum and photoreactions of halorhodopsin, Biochim. Biophys. Acta 682 (1982) 446-451.

[12] J.K. Lanyi, Photochromism of halorhodopsin. *cis/trans* isomerization of the retinal around the 13-14 double bond, J. Biol. Chem. 261 (1986) 14025-14030.

[13] G. Váró, L. Zimányi, X. Fan, L. Sun, R. Needleman, J.K. Lanyi, Photocycle of halorhodopsin from *Halobacterium salinarium*, Biophys. J. 68 (1995) 2062-2072.

[14] B. Scharf, M. Engelhard, Blue halorhodopsin from *Natronobacterium pharaonis*: wavelength regulation by anions, Biochemistry 33 (1994) 6387-6393.

[15] G. Váró, L.S. Brown, J. Sasaki, H. Kandori, A. Maeda, R. Needleman, J.K. Lanyi,

Light-driven chloride ion transport by halorhodopsin from *Natronobacterium pharaonis*. I. The photochemical cycle, Biochemistry 34 (1995) 14490-14499.

[16] N. Kamo, N. Hazemoto, Y. Kobatake, Y. Mukohata, Light and dark adaptation of halorhodopsin, Arch. Biochem. Biophys. 238 (1985) 90-96.

[17] M. Kolbe, H. Besir, L.O. Essen, D. Oesterhelt, Structure of the light-driven chloride pump halorhodopsin at 1.8 Å resolution, Science 288 (2000) 1390-1396.

[18] W. Gmelin, K. Zeth, R. Efremov, J. Heberle, J. Tittor, D. Oesterhelt, The crystal structure of the L1 intermediate of halorhodopsin at 1.9 Å resolution, Photochem. Photobiol. 83 (2007) 369-377.

[19] T. Kouyama, S. Kanada, Y. Takeguchi, A. Narusawa, M. Murakami, K. Ihara, Crystal structure of the light-driven chloride pump halorhodopsin from *Natronomonas pharaonis*, J. Mol. Biol. 396 (2010) 564-579.

[20] M. Rüdiger, D. Oesterhelt, Specific arginine and threonine residues control anion binding and transport in the light-driven chloride pump halorhodopsin, EMBO J. 16 (1997) 3813-3821.

[21] I. Chizhov, M. Engelhard, Temperature and halide dependence of the photocycle of halorhodopsin from *Natronobacterium pharaonis*, Biophys. J. 81 (2001) 1600-1612.

[22] A. Duschl, J.K. Lanyi, L. Zimányi, Properties and photochemistry of a halorhodopsin from

the haloalkalophile, *Natronobacterium pharaonis*, J. Biol. Chem. 265 (1990) 1261-1267.

[23] K. Shimono, M. Iwamoto, M. Sumi, N. Kamo, Functional expression of *pharaonis* phoborhodopsin in *Escherichia coli*, FEBS Lett. 420 (1997) 54-56.

[24] I.P. Hohenfeld, A.A. Wegener, M. Engelhard, Purification of histidine tagged bacteriorhodopsin, *pharaonis* halorhodopsin and *pharaonis* sensory rhodopsin II functionally expressed in *Escherichia coli*, FEBS Lett. 442 (1999) 198-202.

[25] M. Sato, T. Kanamori, N. Kamo, M. Demura, K. Nitta, Stopped-flow analysis on anion binding to blue-form halorhodopsin from *Natronobacterium pharaonis*: comparison with the anion-uptake process during the photocycle, Biochemistry 41 (2002) 2452-2458.

[26] M. Sato, T. Kikukawa, T. Araiso, H. Okita, K. Shimono, N. Kamo, M. Demura, K. Nitta, Roles of Ser130 and Thr126 in chloride binding and photocycle of *pharaonis* halorhodopsin, J. Biochem. (Tokyo) 134 (2003) 151-158.

[27] M. Sato, T. Kikukawa, T. Araiso, H. Okita, K. Shimono, N. Kamo, M. Demura, K. Nitta, Ser-130 of *Natronobacterium pharaonis* halorhodopsin is important for the chloride binding, Biophys. Chem. 104 (2003) 209-216.

[28] M. Sato, M. Kubo, T. Aizawa, N. Kamo, T. Kikukawa, K. Nitta, M. Demura, Role of putative anion-binding sites in cytoplasmic and extracellular channels of *Natronomonas pharaonis* halorhodopsin, Biochemistry 44 (2005) 4775-4784.

[29] M. Shibata, Y. Saito, M. Demura, H. Kandori, Deprotonation of Glu234 during the photocycle of *Natronomonas pharaonis* halorhodopsin, Chem. Phys. Lett. 432 (2006) 545-547.

[30] C. Hasegawa, T. Kikukawa, S. Miyauchi, A. Seki, Y. Sudo, M. Kubo, M. Demura, N. Kamo, Interaction of the halobacterial transducer to a halorhodopsin mutant engineered so as to bind the transducer: Cl^- circulation within the extracellular channel, Photochem. Photobiol. 83 (2007) 293-302.

[31] Y. Furutani, M. Ito, Y. Sudo, N. Kamo, H. Kandori, Protein-protein interaction of a *pharaonis* halorhodopsin mutant forming a complex with *pharaonis* halobacterial transducer protein II detected by Fourier-transform infrared spectroscopy, Photochem. Photobiol. 84 (2008) 874-879.

[32] K. Inoue, M. Kubo, M. Demura, N. Kamo, M. Terazima, Reaction dynamics of halorhodopsin studied by time-resolved diffusion, Biophys. J. 96 (2009) 3724-3734.

[33] M. Kubo, T. Kikukawa, S. Miyauchi, A. Seki, M. Kamiya, T. Aizawa, K. Kawano, N. Kamo, M. Demura, Role of Arg123 in light-driven anion pump mechanisms of *pharaonis* halorhodopsin, Photochem. Photobiol. 85 (2009) 547-555.

[34] T. Sasaki, M. Kubo, T. Kikukawa, M. Kamiya, T. Aizawa, K. Kawano, N. Kamo, M. Demura, Halorhodopsin from *Natronomonas pharaonis* forms a trimer even in the presence

of a detergent, dodecyl-β-D-maltoside, Photochem. Photobiol. 85 (2009) 130-136.

[35] M. Rüdiger, U. Haupts, K. Gerwert, D. Oesterhelt, Chemical reconstitution of a chloride pump inactivated by a single point mutation, EMBO J. 14 (1995) 1599-1606.

[36] K.-H. Jung, E.N. Spudich, V.D. Trivedi, J.L. Spudich, An archaeal photosignal-transducing module mediates phototaxis in *Escherichia coli*, J. Bacteriol. 183 (2001) 6365-6371.

[37] M.P. Krebs, E.N. Spudich, J.L. Spudich, Rapid high-yield purification and liposome reconstitution of polyhistidine-tagged sensory rhodopsin I, Protein expression purif. 6 (1995) 780-788.

[38] B. Perazzona, E.N. Spudich, J.L. Spudich, Deletion mapping of the sites on the HtrI transducer for sensory rhodopsin I interaction, J. Bacteriol. 178 (1996) 6475-6478.

[39] K. Shimono, Y. Ikeura, Y. Sudo, M. Iwamoto, N. Kamo, Environment around the chromophore in *pharaonis* phoborhodopsin: mutation analysis of the retinal binding site, Biochim. Biophys. Acta 1515 (2001) 92-100.

[40] R.A. Bogomolni, M.E. Taylor, W. Stoeckenius, Reconstitution of purified halorhodopsin, Proc. Natl. Acad. Sci. USA 81 (1984) 5408-5411.

[41] A. Duschl, M.A. McCloskey, J.K. Lanyi, Functional reconstitution of halorhodopsin. Properties of halorhodopsin-containing proteoliposomes, J. Biol. Chem. 263 (1988) 17016-17022.

[42] M. Steiner, D. Oesterhelt, Isolation and properties of the native chromoprotein halorhodopsin, EMBO J. 2 (1983) 1379-1385.

[43] S. Karnik, T. Doi, R. Molday, H.G. Khorana, Expression of the archaebacterial bacterio-opsin gene with and without signal sequences in *Escherichia coli*: the expressed proteins are located in the membrane but bind retinal poorly, Proc. Natl. Acad. Sci. USA 87 (1990) 8955-8959.

[44] N. Kamo, T. Hashiba, T. Kikukawa, T. Araiso, K. Ihara, T. Nara, A light-driven proton pump from haloterrigena turkmenica: functional expression in *Escherichia coli* membrane and coupling with a H^+ co-transporter, Biochem. Biophys. Res. Commun. 341 (2006) 285-290.

[45] Y. Sugiyama, Y. Mukohata, Isolation and characterization of halorhodopsm from *Halobacterium halobium*, Journal of Biochemistry 96 (1984) 413.

[46] T. Sasaki, T. Aizawa, M. Kamiya, T. Kikukawa, K. Kawano, N. Kamo, M. Demura, Effect of chloride binding on the thermal trimer - monomer conversion of halorhodopsin in the solubilized system, Biochemistry 48 (2009) 12089-12095.

[47] M. Steiner, D. Oesterhelt, M. Ariki, J.K. Lanyi, Halide binding by the purified halorhodopsin chromoprotein. I. Effects on the chromophore, J. Biol. Chem. 259 (1984) 2179-2184.

Figure Legends

Figure 1. The expression and purification of HsHR in *E. coli* cells. (A) SDS-PAGE analyses of whole-cell extracts from 1, BL21(DE3) and 2, Rosetta(DE3) harboring HsHR expression plasmid. Protein bands were visualized using InVision His-tag in-gel stain. The band corresponding to HsHR (marked by an arrow) only appeared in the lane of Rosetta(DE3). (B) Flash-induced transient absorption changes of *E. coli* cells harboring the expression plasmids of NpHR (upper) and HsHR (lower). No photoactivity was observed for HsHR/Rosetta (DE3). The transient absorption changes at 580 nm reflect the recoveries of the photolyzed HRs to the original states. (C) Western blot analyses using anti His-Tag antibody of Rosetta(DE3) cell fractions expressing HsHR and the purified HsHR. Lane 1, whole-cell extract; lane 2, insoluble fraction after low-speed centrifugation of the cellular lysate; lanes 3 and 4, soluble and membrane fractions, respectively, separated by ultra-centrifugation of the remaining supernatant; lane 5, purified HsHR by Ni-chelating chromatography after DDM-solubilization in the presence of 500 μM all-*trans* retinal. (D) Absorption spectrum of this purified HsHR. The protein has been light-adapted by yellow light and dissolved in 10 mM citrate, pH 5.0, including 500 mM NaCl and 0.1% DDM.

Figure 2. Bleaching rates of NpHR and HsHR purified from *E. coli* membranes under continuous illumination. Relative concentrations of unbleached (alive) NpHR (○) and HsHR (●) were estimated from the absorbances at λ_{max}s and plotted versus the illumination duration. Buffer solution was 10

mM MES, pH 6.0, including 0.1% DDM. The samples were irradiated with yellow light at 20 °C.

Figure 3. Visible CD spectra (A) and gel filtration chromatography (B) of HsHR purified from *E. coli* membranes. Buffer solutions were 10 mM MES, pH 6.0, including 300 mM NaCl and 0.1% DDM. Before CD measurement, HsHR was light-adapted by yellow light. For the chromatographs, the elutions of HRs were monitored at 580 nm. The respective measurements were performed at 25 °C for (A) and at room temperature for (B).

Figure 4. Chloride-dependent changes in the absorption spectrum of HsHR obtained from *E. coli* membrane. The spectral changes (A), the corresponding difference spectra (B) and the amplitude change at 577 nm (C) are shown, respectively. Before each spectral measurement, HsHR was light-adapted by yellow light. Buffer solutions were 10 mM citrate, pH 5.0, including 0.1% DDM and the appropriate amount of NaCl. The ionic strengths were kept constant and equivalent to 4 M NaCl by the addition of Na_2SO_4. Concentrations of Cl^- were 0, 0.2, 0.5, 1, 2, 4, 6, 8, 10, 20, 100, 500, and 1000 mM. The arrows indicate a spectral shift by the addition of Cl^-. In (C), the absorption changes were normalized to a scale between zero in sulfate and one in 1 M chloride. Here, the solid line denotes the best-fitted result with a 0.82 order binding of chloride at the dissociation constant of 2.6 mM.

Figure 5. The light-dark adaptation of HsHR purified from *E. coli* membrane. Illumination dependent changes were observed in the absorption spectrum (A) and HPLC-analyzed retinal isomer compositions (B). The terms “Dark” and “Light” in the panels indicate those obtained using dark- and light-adapted samples, respectively. Buffer solutions were 10 mM MES, pH 6.0, including 4 M NaCl and 0.1% DDM. The peaks correspond to 1, all-*trans* 15-*syn*; 2, 13-*cis* 15-*syn*; 3, 13-*cis* 15-*anti*; 4, all-*trans* 15-*anti.*

Figure 6. Comparison of flash-induced absorbance changes between DDM-solubilized HsHR from *E. coli* membrane and HsHR in the native membrane. The data at (A) 4 M NaCl and (B) 1.33 M Na_2SO_4, are shown in the time-resolved difference spectra (left column) and transient absorption changes at typical wavelengths (right column). Here, the terms "*E.coli*" and "*H. salinarum*" in the panels denote the samples, "DDM-solubilized HsHR purified from *E. coli* membrane" and "HsHR in *H. salinarum* membrane", respectively. Before the measurements, each sample was light-adapted by yellow light. Buffer solutions for the DDM-solubilized HsHR were 10 mM MES, pH 6.0, including 0.1% DDM and the indicated salt. Buffer solutions for HsHR in the native membrane included 0.5% Tween-20 instead of 0.1% DDM for the solubilized HsHR. The time-resolved difference spectra were shown in a logarithmic time intervals from 0.01 to 130 msec. Here, the spectrum at 0.01 ms

was highlighted in a gray thick line. The transient absorption changes at three selected wavelengths reflect the formation and decay of the representative intermediates and the recovery of the initial ground state. All measurements were performed at 20 °C.

Figure 7. Light-induced pH changes of asolectin liposomes containing HsHR from *E. coli* membrane. The gray bar indicates the period of illumination by orange light (590 ± 8.5 nm). The liposomes were suspended in 0.1 mM MES, pH 6.0, including 1 M NaCl and 50 μM CCCP. The right trace was obtained after the addition of 1% DDM. The measurements were performed at room temperature.

Figure 1

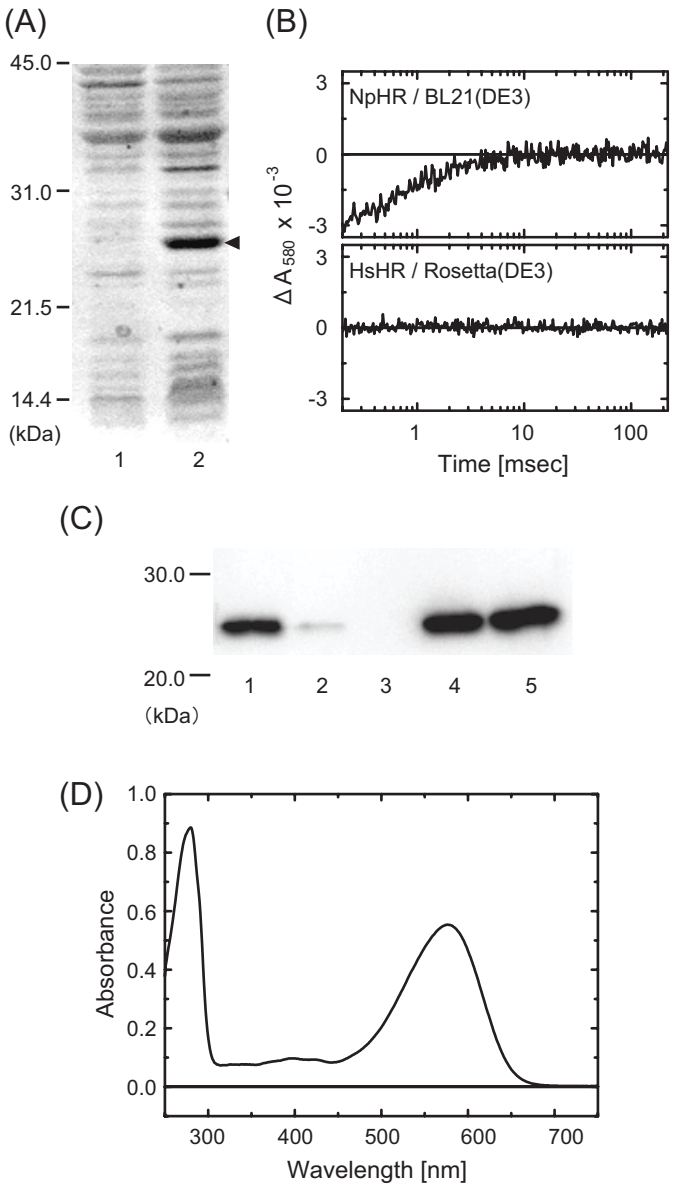
(A)
45.0
31.0
21.5
14.4
(kDa)
1
2
(B)
NpHR / BL21(DE3)
HsHR / Rosetta(DE3)
ΔA580 x 10-3
3
0
-3
1
10
100
Time [msec]
(C)
30.0
20.0
(kDa)
1
2
3
4
5
(D)
Absorbance
1.0
0.8
0.6
0.4
0.2
0.0
300
400
500
600
700
Wavelength [nm]

Figure 2

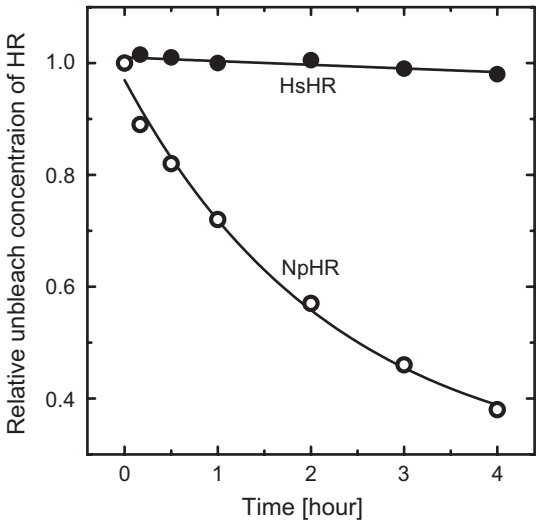
Relative unbleach concentraion of HR
1.0
0.8
0.6
0.4
HsHR
NpHR
0
1
2
3
4
Time [hour]

Figure 3

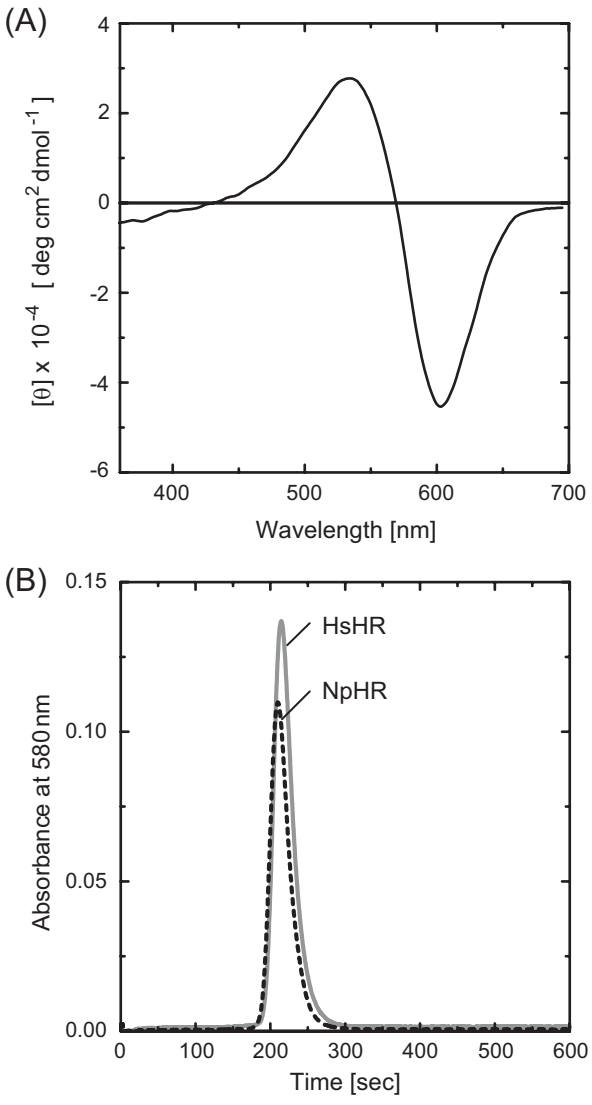
(A)
4
2
0
-2
-4
-6
[θ] x 10^-4 [deg cm^2 dmol^-1]
400
500
600
700
Wavelength [nm]
(B)
0.15
0.10
0.05
0.00
Absorbance at 580 nm
HsHR
NpHR
0
100
200
300
400
500
600
Time [sec]

Figure 4

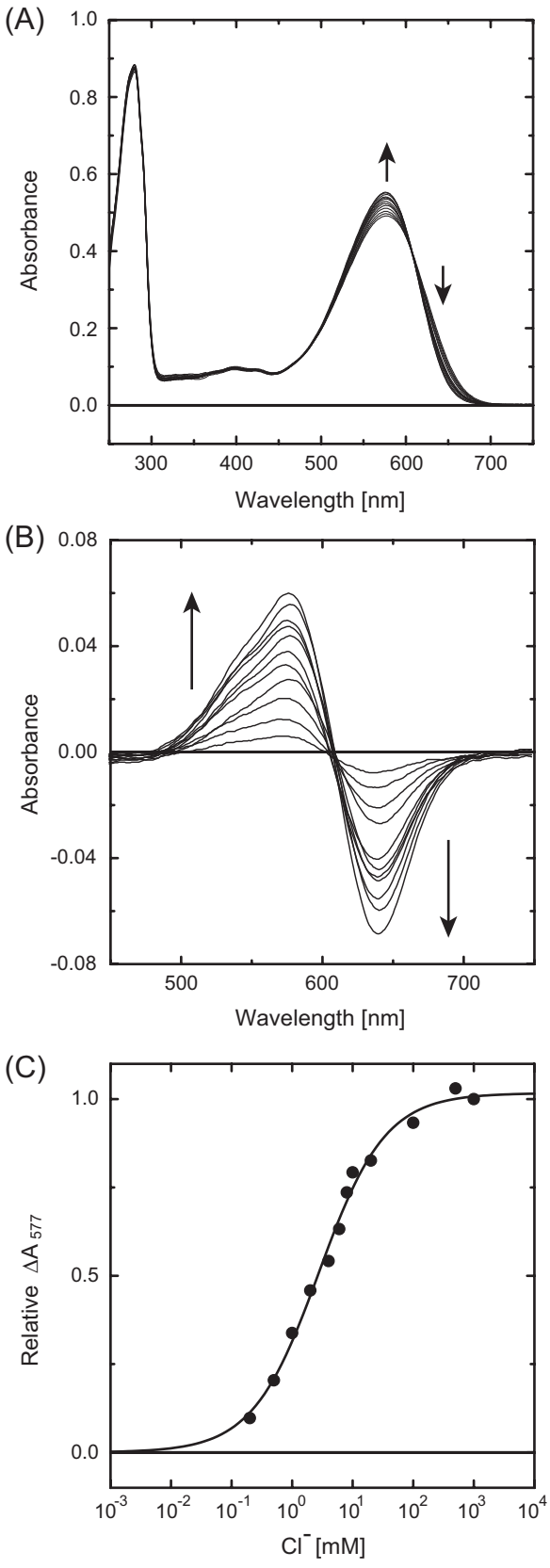
(A)
1.0
0.8
0.6
0.4
0.2
0.0
Absorbance
300
400
500
600
700
Wavelength [nm]
(B)
0.08
0.04
0.00
-0.04
-0.08
Absorbance
500
600
700
Wavelength [nm]
(C)
1.0
0.5
0.0
Relative ΔA577
10-3
10-2
10-1
100
101
102
103
104
Cl- [mM]

Figure 5

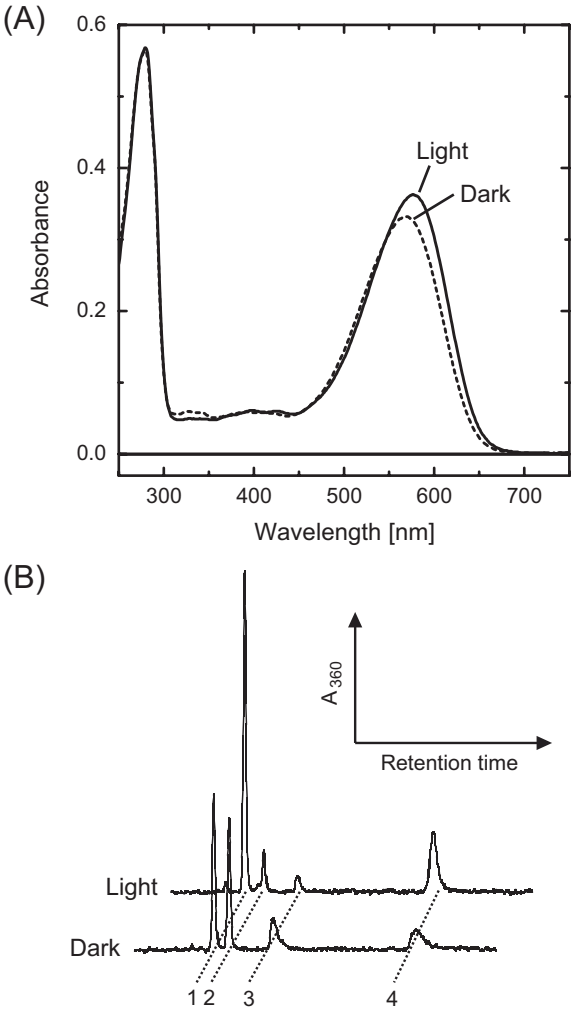
(A)
0.6
0.4
0.2
0.0
Absorbance
Light
Dark
300
400
500
600
700
Wavelength [nm]
(B)
A360
Retention time
Light
Dark
1 2
3
4

Figure 6

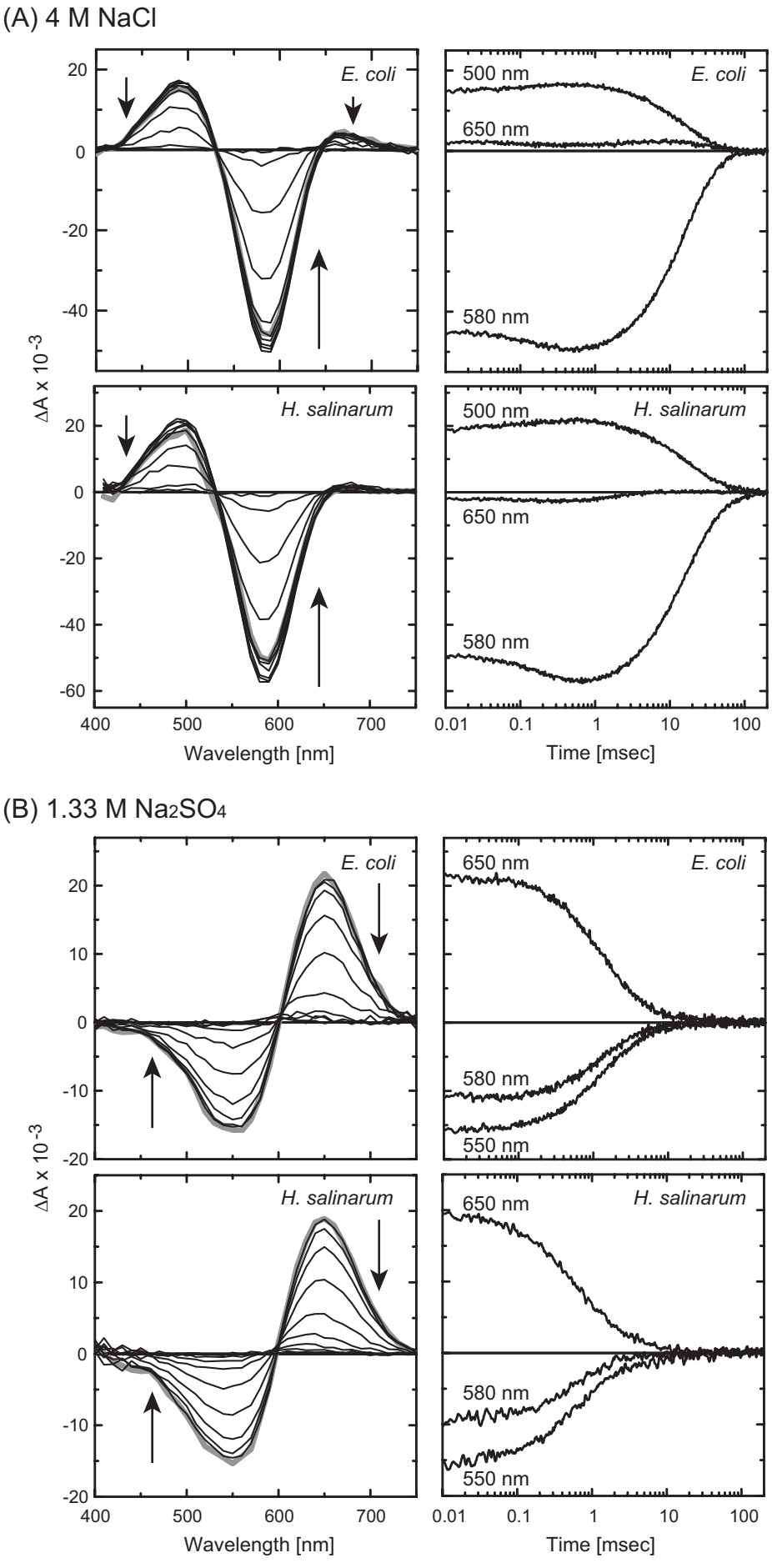
(A) 4 M NaCl
E. coli
500 nm
650 nm
580 nm
H. salinarum
ΔA x 10-3
Wavelength [nm]
Time [msec]
(B) 1.33 M Na2SO4
550 nm

Figure 7